APS March Meeting

Application of Clifford algebra and quaternion representations to (3+1)D non-destructive testing

Sadataka Furui^A and Serge Dos Santos^B
A: Teikyo Univ. Faculty of Science and Engineering, Utsunomiya 320 Japan
B: INSA Centre Val de Loire,UMR 1253,Imaging and Brain:iBraiN,Inserm,
3 rue dela Chocolade, CS 23410-F-41034 Blois Cedex, France

APS March Meeting

1. Introduction
2. Fixed point lattice action of phonetic waves in Weyl fermion sea
3. Clifford algebra of $A_{3,1}$
4. Numerical calculations of hysteresis effects in quarternion basis model

5 Conclusion and discussion

TEIKYO

INSA INSTITUT NATIONAL DES SCIENCES APPLIQUÉES CENTRE VAL DE LOIRE

1. Introduction

1. Introduction

- In signal and image processings quaternions, hypercomplex numbers expressed as $q = q_0 + q_1\mathbf{i} + q_2\mathbf{j} + q_3\mathbf{k}$, where $\mathbf{i}^2 = \mathbf{j}^2 = \mathbf{k}^2 = \mathbf{ijk} = -1$, $\mathbf{ij} = -\mathbf{ji} = \mathbf{k}$, $\mathbf{jk} = -\mathbf{kj} = \mathbf{i}$, $\mathbf{ki} = -\mathbf{ik} = \mathbf{j}$ are used. For a reference, see Miran et al. (2023).

- In time reversal based nonlinear elastic wave spectroscopy (TR-NEWS), convolutions of an ultrasonic wave and its time reversed (TR) ultrasonic wave are measured, and position of anomalous scattering positions are searched.

  Recent progress of non-destructive testing (NDT) using ultrasonic wave is reviewed in Dvorkava et al.(2023). For application in medical investigation, Classification of Difffeent Source(CDS) and Classification of Different Positions(CDP) techniques are presented. For measuring the Hellinger divergence of CDS and CDP of nonlinearly scattered ultrasonic waves, the pulse inversion method was used.

- The CDP experiment was done in spacial 3 dimensions and the successful techniques utilized in spacial 2 dimensions need to be extended. A review on TR-NEWS in (2+1)D including hysteresis effects using Excitation Symmetry Analysis Model(ESAM) proposed by Dos Santos and Plag (2007) and the decomposition of the time reversal operator (DORT) proposed by Prada and Fink (1998) is given in Goursolle et al.(2007) and Dos Santos (2010).

- Rajpoot et al.(2009) discuss 3D echocardiography images using Riesz filter. The 3D image $f(x, y, z)$ is multiplied by spacially isotropic time-independent filter and integrated. Using the freedom of choice of periphery of a volume $\partial V = d\mu$, and the Radon's theorem $F(\partial V) = \int_{\partial V} f(x, y, z)d\mu$, $f = dF/d\mu$ is applied for improving the 3D image recognition.

  For medical applications, it is important to measure time dependent hysteresis effects.

2. Fixed point lattice action of phonetic waves in Weyl fermion sea

2. Fixed point lattice action of phonetic waves in Weyl fermion sea

- For the lattice simulatiion of propagation of ultrasonic wave in materials, we replace Dirac fermions to Weyl fermions expressed by quaternions. Since the ultrasonic waves are expressedby the third order polynomials $x(t)$, $x^2(t)$ and $x^3(t)$, we assign amplitudes of these component to imaginary part of quaternions.

- The lattice simulation of ultrasonic waves in materials are done by modifying fixed point (FP) actions proposed by deGrand et al. (1998) in quantum chromodynamics (QCD). Restricting the path length less than or equal to 8 lattice units, they considered 28 paths. We omit the path that runs on a periphery of a unit plaquette twice. We search the optimal weight function of the 27 paths, that yield the minimal action. For optimization, we adopt the machine learning (ML) techniques.

- Paths on a 2D plane, which are called A type, consist of 7 paths.

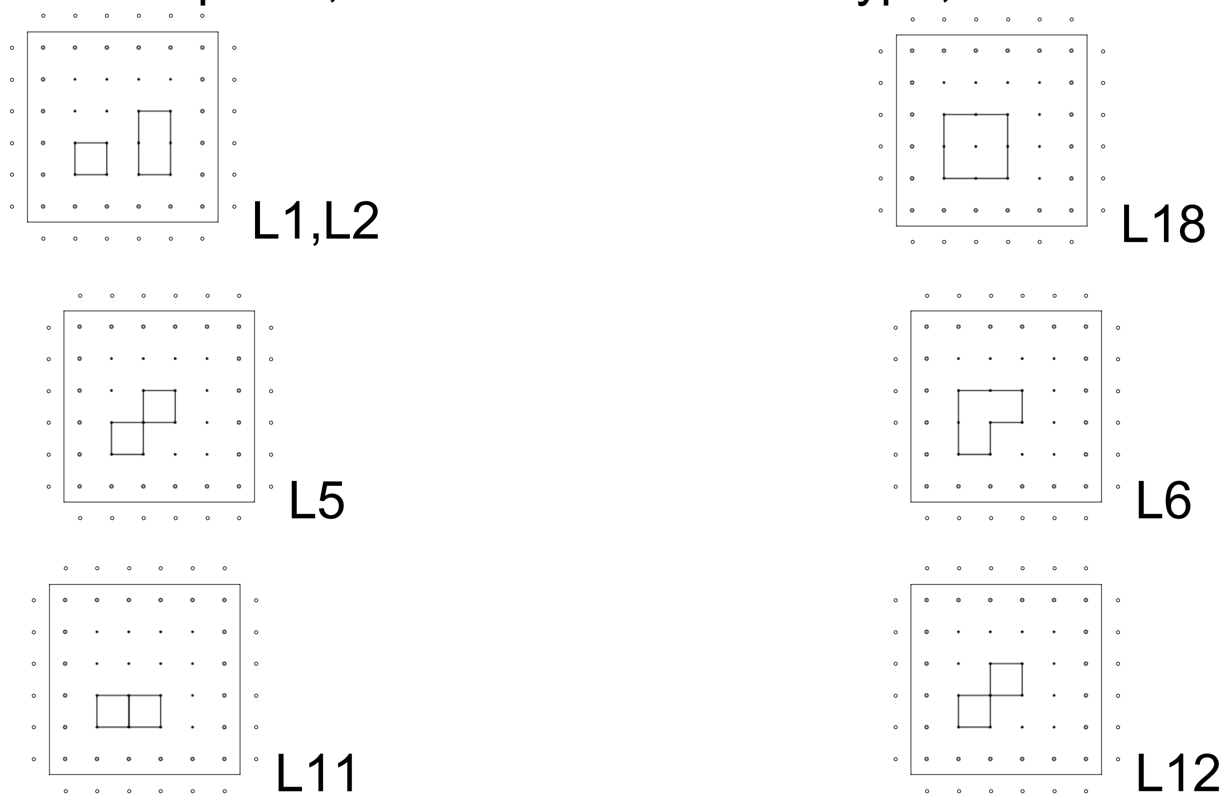

Fig.1 The $L1,\ L2,\ L18$,$L5,\ L6$ and $L11,\ L12$ on 2D planes.

- The B type loops consists of paths on a 2D plane and on another plane expanded by e_1 and e_2 connected by two parallel paths along $e_1 \wedge e_2$. The simplest path $L3$ is indicated in Fig. 2. The path from lower plane to upper plane is denoted by a blue circle and the opposite direction is denoted by a red circle. The first step on a 2D plane is one lattice unit along e_1,

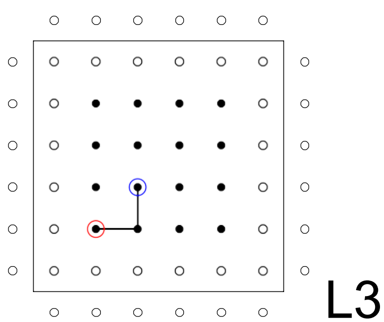

Fig.2 The $L3$ loop on a (2+1)D lattice space.

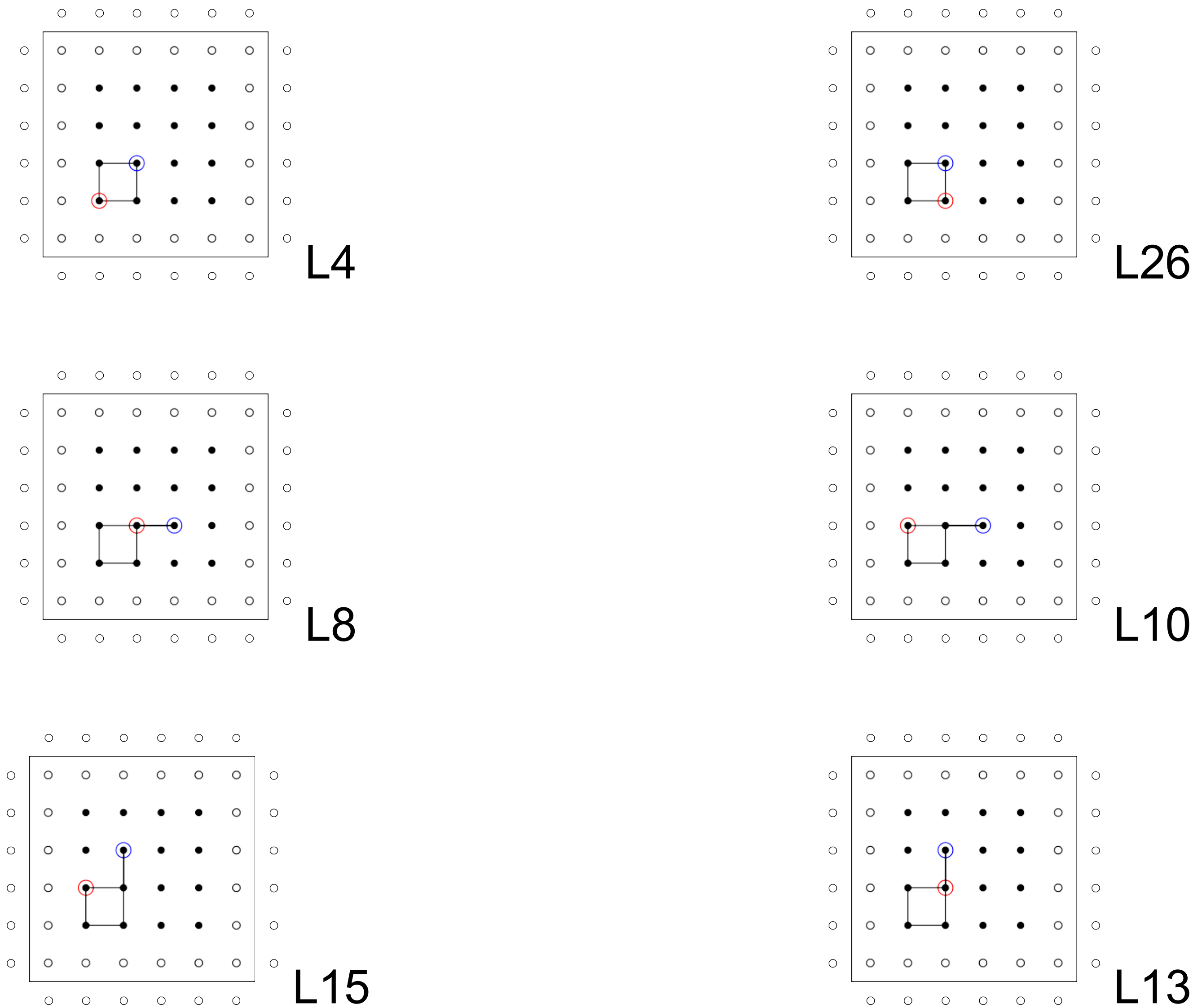

Fig.3. Link paths $L4$, $L26$, $L8$, $L10$, $L15$, $L13$.

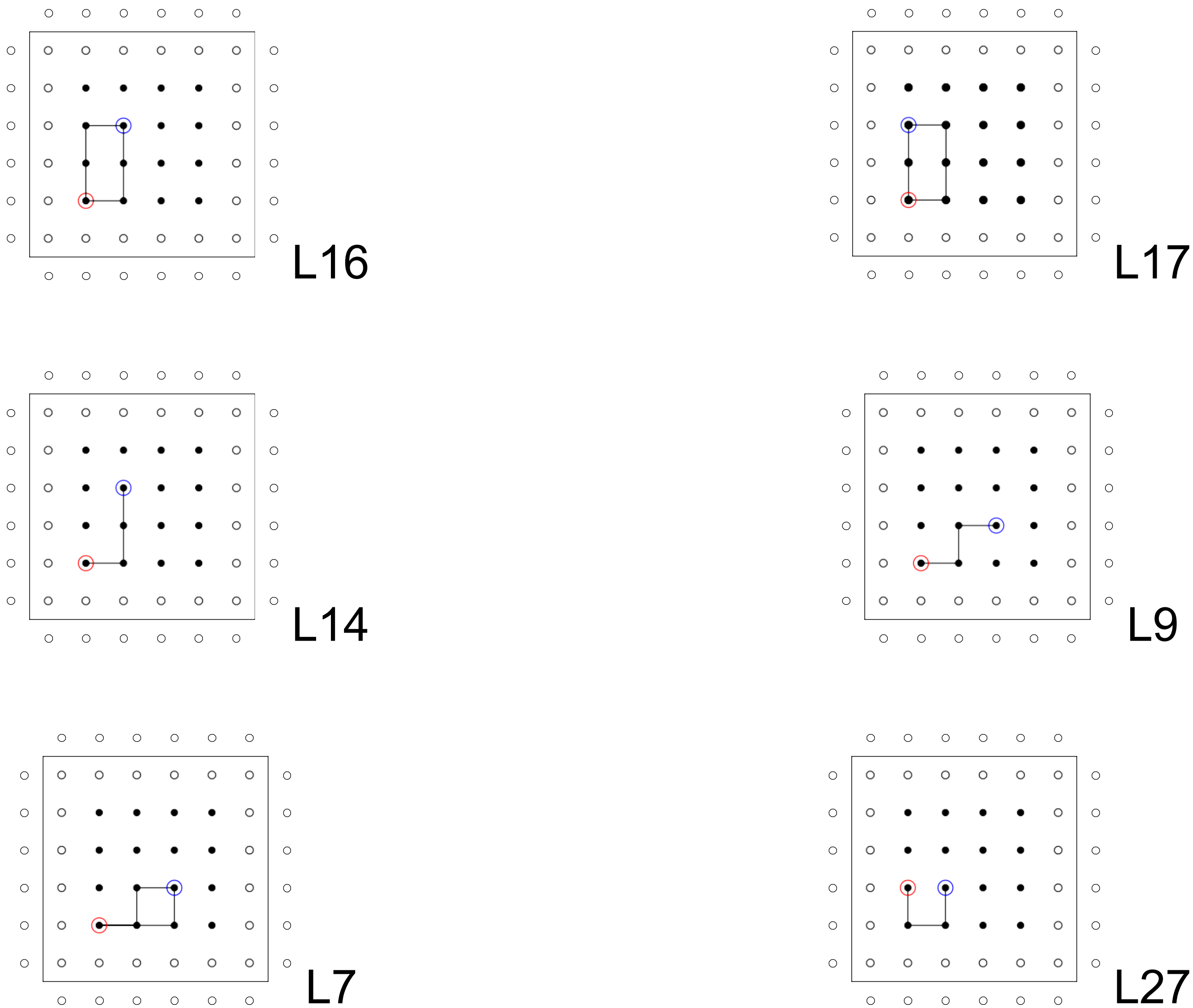

Fig.4. Link paths $L16$, $L17$, $L14$, $L9$, $L7$, $L27$.

- There are 7 paths in the $(3+1)D$ whose length are (6+2) lattice units

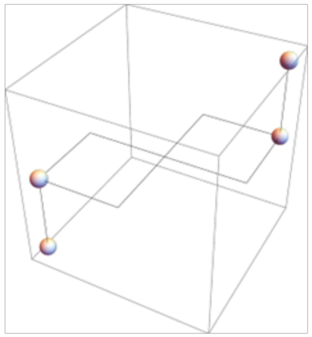
L19

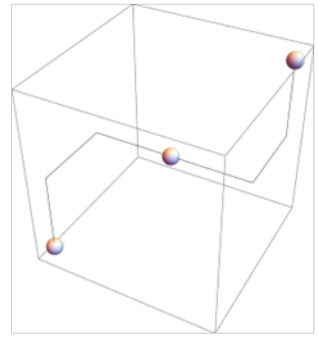
L20

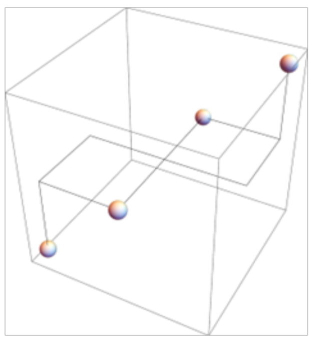
L21

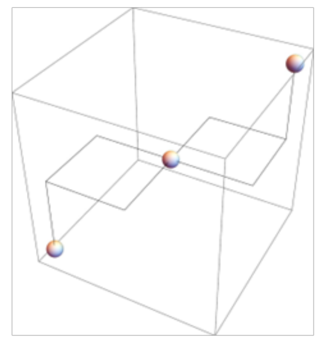
L22

Fig.5 The path of $L19, L20, L21, L22$. Balls are positions that time shifts occur. The origin and the end of the path is the left lower corner.

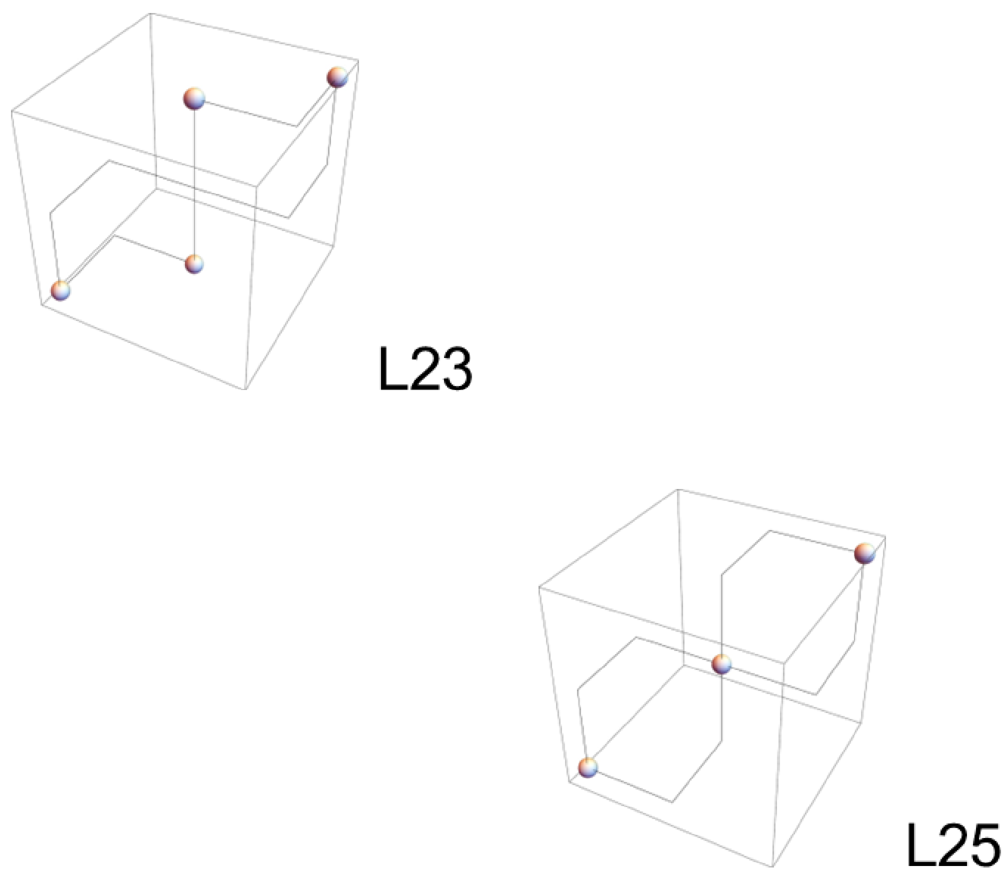

Fig.6 The path of $L23, L24, L25$. Balls are positions that time shifts occur. The origin and the end of the path is the left lower corner.

3. Clifford algebra of $\mathcal{A}_{3,1}$

3. Clifford algebra of $\mathcal{A}_{3,1}$.

- Up to (2+1)D, quaternion basis model can be constructed by introducing linear combinations of quaternions H, but in (3+1)D, we need to introduce biquaternions. The mapping $j : \mathrm{R}^{3,1} \to M_2(\mathrm{H})$ proposed by Garling (2011) is

$$j(\mathcal{A}_{3,1}^{+}) = \begin{pmatrix} a_1 + a_2\mathrm{k} & b_1\mathrm{i} + b_2\mathrm{j} \\ c_1\mathrm{i} + c_2\mathrm{j} & d_1 + d_2\mathrm{k} \end{pmatrix},$$

  where $a_i, b_i, c_i, d_i \quad (i = 1, 2)$ are real.

- The basis of a biquaternion is expressed as $e_i e_j = \epsilon^{ijk} e_k$, where ϵ^{ijk} is ± 1 depending on cyclic order of $ij \leq 3$. $e_1 \sim x$, $e_2 \sim y$, $e_3 \sim z$ and $e_i e_4 \sim t$, for $i \leq 3$. (There are 3 quaternion local times.)

- The sequences of $e_i e_j$ and $e_k e_l$ at each step, including the end and step 0, is chosen such as one of i or j equals one of k or l.

L19,L20,L25

1	2	3	4	5	6	7	8	9	10	11	12	13	14	15	16
x	y	z	t	-z	-t	-x	-y	-x	-y	-z	-t	z	t	x	y
23	31	12	24	-12	-24	-23	-31	-23	-31	-12	-24	12	24	23	31
x	y	z	t	-z	-y	-x	-t	-x	-y	-z	-t	z	y	x	t
23	31	12	24	-12	-31	-23	-24	-23	-31	-12	-24	12	31	23	24
x	y	z	t	-x	-y	-z	-t	-x	-y	-z	-t	x	y	z	t
23	31	12	24	-23	-13	-12	-24	-23	-31	-12	-24	23	13	12	24

Table 1. Directions of the wave front of loops L19, L20, L25

L21 ,L22, L23, L24

1	2	3	4	5	6	7	8	9	10	11	12	13	14	15	16
x	y	z	t	-z	-x	-t	-y	-x	-y	-z	-t	z	x	t	y
23	31	12	14/24	-12	-23	-34	-13	-23	-31	-12	-14/24	12	23	34	13
x	y	z	t	-z	-x	-y	-t	-x	-y	-z	-t	z	x	y	t
23	31	12	14/24	-12	-23	-31	-34	-23	-31	-12	-14/24	12	23	31	34
x	y	z	t	-y	-x	-t	-z	-x	-y	-z	-t	y	x	t	z
23	31	12	14	-31	-23	-24	-12	-23	-31	-12	-14	31	23	24	12
x	y	z	t	-y	-x	-z	-t	-x	-y	-z	-t	y	x	z	t
23	31	12	14	-31	-23	-12	-24	-23	-31	-12	-14	31	23	12	24

Table 2 . Directions of the wave front of loops $L21, L22, L23, L24$

- Porteous (1995) derived actions in $\mathcal{A}_{2,1}$ from eigenvalues of the matrix $\begin{pmatrix} x & xx^- \\ 1 & x^- \end{pmatrix}$ sandwiched by the Vahlen matrices(1901).

- Its transformation can be expressed as

$$\begin{pmatrix} a & c \\ b & d \end{pmatrix}\begin{pmatrix} x & xx^- \\ 1 & x^- \end{pmatrix}\begin{pmatrix} d^- & c^- \\ b^- & a^- \end{pmatrix} = \lambda\begin{pmatrix} x' & x'x'^- \\ 1 & x' \end{pmatrix}.$$

  We interplet real eigenvalue $\lambda = (bx+d)(bx+d)^-$ yields the plaquette action and xx^- yields the link action.

- The matrix $\begin{pmatrix} a & c \\ b & d \end{pmatrix}$ represents a special conformal transformation.

- In analogy to the $(2+1)D$ case, one could map x, y, z, t on S^4 as

$$X = \frac{2u_1}{1+|u|^2}e_1 + \frac{2u_2}{1+|u|^2}e_2 + \frac{2u_3}{1+|u|^2}e_3 + \frac{1-|u|^2}{1+|u|^2}e_4.$$

where $|u|^2 = u_1^2 + u_2^2 + u_3^2$.

- We define a reflection matrix ref $= \begin{pmatrix} 0 & 0 & 1 & 0 \\ 0 & 0 & 0 & -1 \\ 1 & 0 & 0 & 0 \\ 0 & -1 & 0 & 0 \end{pmatrix}$ and define $\bar{e}_i = -$ref.e_i $(i = 1, \cdots, 4)$. For $i = 1, 2, 3$ $e_i.\bar{e}_i = \begin{pmatrix} 0 & I_2 \\ -I_2 & 0 \end{pmatrix}$ and $e_4.\bar{e}_4 = \begin{pmatrix} 0 & -I_2 \\ I_2 & 0 \end{pmatrix}$.

- The sum of the products $e_i\bar{e}_i + \bar{e}_i e_i$ is 0 due to anticommutativity of quaternions. Following the conformal treatment of Clifford algebra of Porteous (1995), we define $\mathcal{X} = \begin{pmatrix} X & X\bar{X} \\ I_4 & \bar{X} \end{pmatrix}$, where I_4 is 4 dimensional diagonal matrix.

- We define $X_1 = \begin{pmatrix} x_1, & x_1\bar{x}_1 \\ I_4 & \bar{x}_1 \end{pmatrix}$, $V_1 = \begin{pmatrix} a_1 I_4 & b_1 e_2 e_3 \\ c_1 e_2 e_3 & 0 \end{pmatrix}$ and $V_1^\dagger = \begin{pmatrix} 0 & c_1 \overline{e_2 e_3} \\ b_1 \overline{e_2 e_3} & a_1 \bar{I}_4 \end{pmatrix}$. Calculate $V_1 X_1 V_1^\dagger - X_1$.

- $X_2 = \begin{pmatrix} x_2, & x_2\bar{x}_2 \\ I_4 & \bar{x}_2 \end{pmatrix}$, $V_2 = \begin{pmatrix} a_1 I_4 + a_2 e_1 e_3 & 0 \\ 0 & d_2 e_1 e_3 \end{pmatrix}$ and $V_1^\dagger = \begin{pmatrix} d_2 \overline{e_1 e_3} & 0 \\ 0 & a_1 \bar{I}_4 + a_2 \overline{e_1 e_3} \end{pmatrix}$. Calculate $V_2 X_2 V_2^\dagger - X_2$.

- $X_3 = \begin{pmatrix} x_3, & x_3\bar{x}_3 \\ I_4 & \bar{x}_3 \end{pmatrix}$, $V_3 = \begin{pmatrix} a_1 I_4 & 0 \\ 0 & d_1 e_i e_4 \end{pmatrix}$ and $V_3^\dagger = \begin{pmatrix} d_1 \overline{e_i e_4} & 0 \\ 0 & a_1 \bar{I}_4 \end{pmatrix}$ $(i = 1, 2$ or $3)$.

  Calculate $V_3 X_3 V_3^\dagger - X_3$.

- We continue up to X_8 or X_{16} and calculate actions.

- After the singular value decomposition (SVD) of eigenvalues of the 4×4 matrices, we obtain two eigenvalues at each steps.

- The eigenvalues of loops $L19, L20, L25$ and $, L21, L22$ with $t = e_2 e_4, e_3 e_4$ are shown in Fig.8. Those of loops $L23, L24$ and $L21, L22$ with $t = e_1 e_4, e_3 e_4$ are shown in Fig.9.

- At fixed i, eigenvalues monotonically increase as j increases as the string theory.

- Actions are calculated by taking the derivative with respect to j at (i, j).

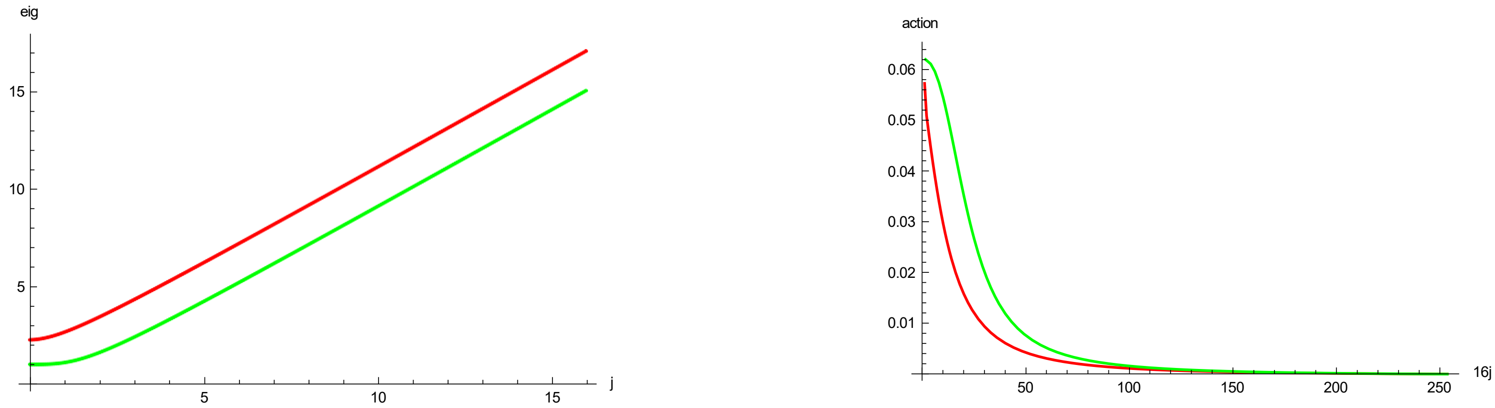

Fig. 8 Eigenvalues (left) and actions (right) of $L19, L20, L25$ and $L21, L22$ with e_2e_4 step 3 after Singular Value Decomposition (SVD). Red points are contribution of large eigenvalues, green points are contribution of small eigenvalues.

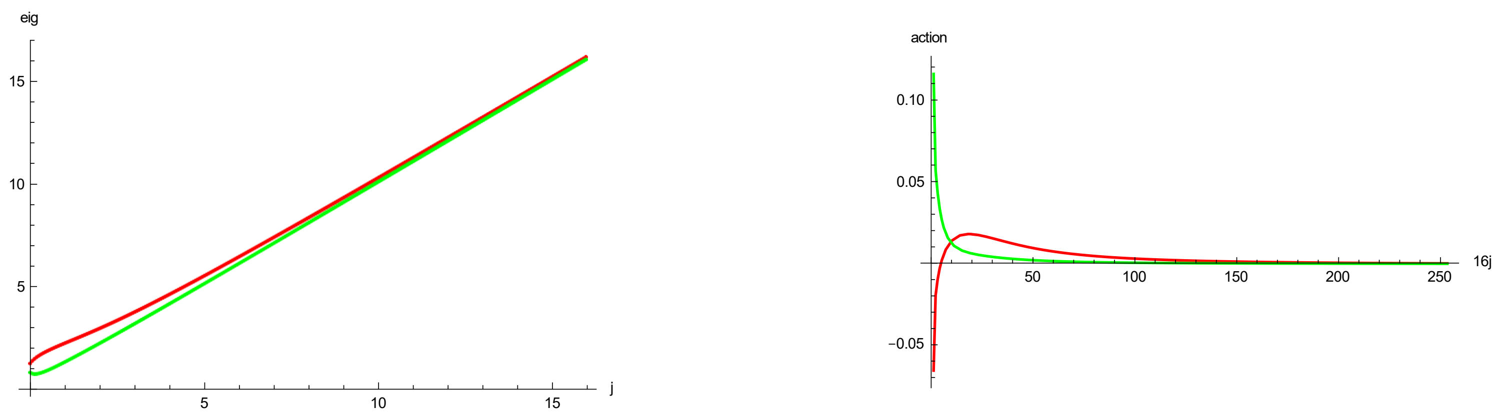

Fig.9 Eigenvalues (left) and actions (right) of $L23, L24$ and $L21, L22$ with e_1e_4 step 3 after SVD. Red lines are the contribution of large eigenvalues, green lines are contribution of small eigenvalues.

Fig.10 The eigenvalues (left) and actions (right) of $L22$ step 12 as a function of $16j = 0, \cdots, 255$

Fig.11 The eigenvalues (left) and actions (right) of $L24$ step 10 as a function of $16j = 0, \cdots, 255$.

4. Numerical calculations of hysteresis effects in quaternion basis model

4. Numerical calculations of hysteresis effects in quarternion basis model

- In R^3, we define $\mathrm{x} =^t (x, y, z)$ and $A[\mathrm{x}] = \begin{pmatrix} 0 & -z & y \\ z & 0 & x \\ -y & x & 0 \end{pmatrix}$.

  When $|\mathrm{x}| = \theta$, Gray et al.(2006) showed that

$$expA[\mathrm{x}] = I + \frac{\sin\theta}{\theta}A[\mathrm{x}] + \frac{1-\cos\theta}{\theta^2}A[\mathrm{x}]^2$$

- A quaternion $\mathrm{q} = a_0e_0 + a_2e_2$ is isomorphic to C.

  A mapping $T_q(q') = qq'$, yields

$$\begin{aligned} T_q(e_0) &= e_0x_{11} + e_2x_{21} \\ T_q(e_2) &= e_0x_{12} + e_2x_{22} \end{aligned}$$

- We choose, following Chevalley (1946) $T_{e_1} = \begin{pmatrix} \sqrt{-1} & 0 \\ 0 & -\sqrt{-1} \end{pmatrix}$.

  A rotation around the x axis of $D_1(\theta) = \begin{pmatrix} 0 & 0 & 0 \\ 0 & \sqrt{-1}\theta & 0 \\ 0 & 0 & -\sqrt{-1}\theta \end{pmatrix}$
  is represented by using a symplectic matrix $P = \begin{pmatrix} 1 & 0 & 0 \\ 0 & \sqrt{-1} & 1 \\ 0 & 1 & \sqrt{-1} \end{pmatrix}$
  as $PD_1(\theta)P^{-1}$.

  The matrix of the rotation around x with a counterclockwise angle $|\mathrm{x}| = \theta$
  equals $R[\mathrm{x}] = \begin{pmatrix} 1 & 0 & 0 \\ 0 & 1 & f_{23}(\theta) \\ 0 & f_{32}(\theta) & 1 \end{pmatrix}$.

  The $f_{23}(\theta)$ and the $f_{32}(\theta)$ shows hysteresis or time-delay effects.

- Mayergoyz (2003) analyzed hysteresis effects by imposing one to one relation between (u, f) space and Preisach (α, β) space. When u increases(decreases) f monotonically increases(decreases).

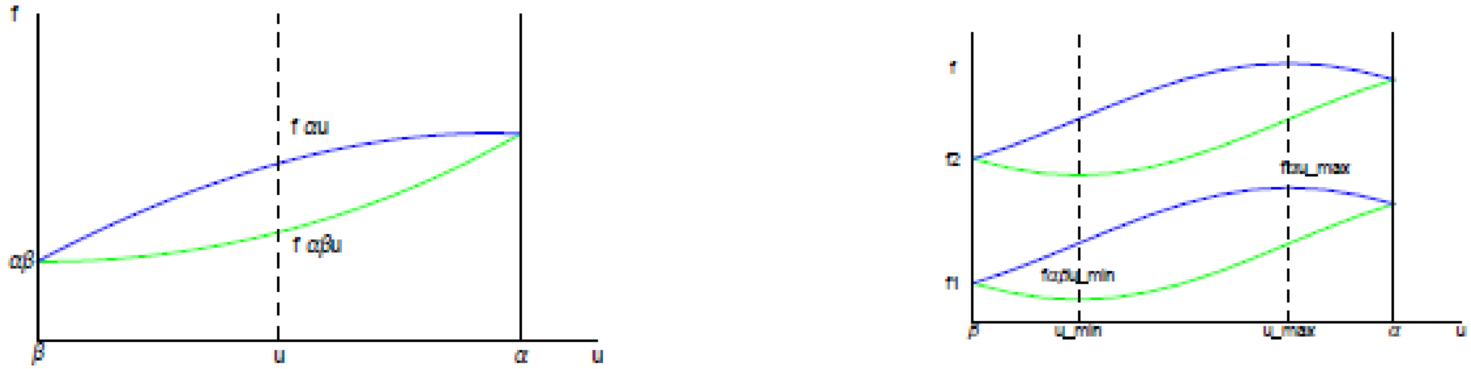

Fig.12 f_{23} (green) and f_{32} (blue) as a function of input u. Left is the Preisach-Mayergoyz model. Right is quaternion basis model.

- We measured the cross-correlation of the ultrasonic wave and its TR wave propsgating in the NOVA university sample, and observed patterns of output f consistent with the quaternion basis model, as shown in Fig.13-16. Depending on the number of layers between the transducer and receiver is even or odd, two peaks or two dips due to the stochastic Markov steps were observed, which can be understood by the theory of Ito (1965).

  Preisach model is valid for low frequency. For ultrasonic wave, the quaternion basis model works.

- In the ESAM, the cross-correlation functions are reduced to the monogenic functions of $E, A, B1$ and $B2$ components.

Fig. 13 Cross-correlation of E_4(left) and E_9 (right) 32001-32050 epochs

Fig. 14 Cross-correlation of A_4(left) and A_9 (right) 32001-32050 epochs

Fig. 15 Cross-correlation of $B1_4$(left) and $B1_9$ (right) 32001-32050 epochs

Fig. 16 Cross-correlation of $B2_4$(left) and $B2_9$ (right) 32001-32050 epochs

- In time reversal mirror (TRM) experiments of Montaldo et al. (2001), responses with two dips and one peak were observed.

5. Conclusion and Discussion

5 Conclusion and discussion

- The NDT of the TR-NEWS using quaternion basis was performed in (2+1)D, and its extension to (3+1)D is continuing. For these data analysis, Cifford algebra of (3+1)D is necessary. We showed that it is possible by extending the model of Porteous(1995). .
  The TR-NEWS of (3+1)D needs biquaternion basis. The present Pulse-inversion basis in ESAM needs to be replaced by quaternion basis.
- For stochastic hysteresis effects, we showed that the quaternion basis model is consistent with experiments of ultrasonic wave propagating in 1 dimension.
  Preisach-Mayergoyz model is valid for low frequency region.
- Similar experiments in (2+1)D and (3+1)D remains for the future.

- The algebra $\mathcal{A}_{4,1}$ is isomorphic to $M_2(\mathrm{H}) \oplus M_2(\mathrm{H})$

$$j(\mathcal{A}_{4,1}) = \begin{pmatrix} x_2\mathrm{i} + x_3\mathrm{j} + x_4\mathrm{k} & -x_1 + x_5 \\ x_1 + x_5 & -x_2\mathrm{i} - x_3\mathrm{j} - x_4\mathrm{k} \end{pmatrix}$$

  where x_i are real.
- In the light front quantization of Srivastava and Brodsky (2001), $\tau = (t - z/c)/\sqrt{2}$ corresponds to $(x_1 - x_5)/\sqrt{2}$. For massless particle, propagators are doubly transverse, i.e. with respect to the gauge direction n_μ and the chilarity direction k_μ.

  The two $M_2(\mathrm{H})$ represent TR symmetric physical fields, and the BRST ghost fields are decoupled.
- In Klebanov's gauge theory (2000), and Chemtob's theory(2022), $S^5 \sim S^2 \times S^3 \sim T^{1,1} \sim S_1^3 \times S_2^3/U(1)$ i.e. product of two quaternions modulus $U(1)$ symmetry.
- Quaternion basis model is promising not only for NDT, but also for light-front quantized QCD.

Thank you for your attention.

References

Miran, S., Flammant, J., Le Bihan, N., Chainais, P. and Brie, D. : Quaternions inSignal and Image Processing, IEEE Signal Processing Magazine, **40** (6) September, pp.26-40. (2023)

Unser, M. Sage, D. and Van De Ville, D.: Multiresolution Monogenic Signal Analysis Using the Riesz-Laplace Wavelet Transform, IEEE Transactions on image Processing, **18** (11) pp.2402-2418 (2009).

Felsberg M. and Sommer, M. : The Monogenic Signal, IEEE Transactions on Signal Processing, **49** (12) pp.3136-3144 (2001).

Rajpoot, K. Grau, V. and Noble, J.A. : Local-phase based 3D boundary detection using monogenic signal and its application to real-time 3-D echography images. IEEE ISBI pp.783-786 (2009)

Kumar, H. ,Parada-Maorga, A. and Ribeiro, A. : Lie Group Algebra Convolutional Filters, arXiv: 2305.04431v1[eess.SP] (2023).

Gaudet, C.J. and Maida, A.: Deep Quaternion Networks, 2018 International Joint Conference on Neural Networks (IJCNN) pp.1-8 IEEE (2018).

Dvorkava, Z., Dos Santos, Serge, Kus, V. and Prevolovsky, Z. : Localization and Classification of scattered nonlinear ultrasonc signatures in biomechanical media using time reversal approach, J. Acoust. Soc. Am. **154** (3) pp.1684-1695 (2023).

Prada, C. and Fink, M. : Separation of interfering acoustic scattered signals using the invariants of the time-reversed operator. Application to Lamb wave characterization, J. Acoust. Soc. Am. **104** (2) pp. 801-807 (1998).

Montaldo, G., Roux, P. Derode, A. , Negeira, C. and Fink, M. :Generation of very high pressure pulses with 1-bit time reversal in a solid waveguide, J. Acoust. Soc. Am **110** (6) pp.2849-2857 (2001).

Goursolle, T., Callé, S. Dos Santos,S. and Bou Matar, O.: A two-dimensional pseudospectral model for time reversal and nonlinear elastic wave spectroscopy, J. Accoust. Soc. Am **122**(6) pp.3220-3229 (2007).

Dos Santos, S. and Plag, C. : Excitation Symmetry Analysis Method (ESAM) for Calculation of Higher Order Nonlinearities, Int. J. Nonlinear Mech. **43** pp 104-119 (2007)

Dos Santos, S. : Analyse des symétries pour un traitement du signal systémique: application à l'imagerie non linéaire des milieux complexes, 10ème Congrès Francais d'Acoustique, Lyon (2010)

Lints, M. Salpere, A. and Dos Santos, S. : Formation and Detection of Solitonic Waves in Dilatant Granular Materials: Potential Application for Nonlinear NDT, NDT.net Issue (2014).

DeGrand, T. Hasenfratz, A., Hasenfratz, P. and Niedermayer, F. : Non-perturbative tests of the fixed point action for SU(3) gauge theory, Nucl. Phys.**B454** 615-637 (1995), arXiv:9506031[hep-lat].

Porteous, L.R. : Clifford Algebras and the Classical Groups, Cambridge University Press (1995).

Garling, D.J.H. : Clifford Algebras: An Introduction, Cambridge University Press (2011).

Vahlen, K.Th. :Ueber Bewegungen und complexe Zahlen, Mathematische Annalen, pp.585-593 (1901).

Gray, A. , Abbena, and Salamon, S. : Modern Differential Geometry of Curves and Surface with Mathematica, Chapman and Hall/CRC, Third Edition (2006).

Chevalley, C. :Theory of Lie Groups, Princeton University Press, Princeton (1946), Asian Text Edition, Overseas Publ. Tokyo (1965).

Ito, K. ;Theory of Probability, (In Japanese) Iwanami Gendai Suugaku **14**, Iwanami Shoten, Tokyo (1965).

Srivastave, P.P. and Brodsky, S.J. : Light-front-quantized QCD in the light-cone gauge: The doubly transverse gauge propagator, Phys. Rev. D **64** 045006 (2001).

Klebanov, L.R. and Tseytlin, A.A. : Gravity Duals of Superstmmetric $SU(N)\times SU(N+M)$ Gauge Theories, Nucl Phys **B578**, 123 (2000) :arXiv hep-th/0002159.

Chemtob, M.: Kaluza-Klein theory for type IIb supergravity on the warped deformed conifold, arXiv: 2209.15503 v1[hep-th].(2022).